

GALNT12 promotes fibrosarcoma growth by accelerating YAP1 nuclear localization

SITE YU*, WENJIE FENG*, JIZHANG ZENG, SITUO ZHOU, YINGHUA PENG and PIHONG ZHANG

Department of Burns and Plastic Surgery, Xiangya Hospital, Central South University, Changsha, Hunan 410008, P.R. China

Received February 22, 2023; Accepted October 17, 2023

DOI: 10.3892/ol.2023.14131

Abstract. Fibrosarcoma is a highly malignant type of soft tissue sarcoma that currently lacks effective treatment options. Polypeptide N-acetylgalactosaminyltransferase 12 (GALNT12) belongs to the uridine diphosphate N-acetylgalactosamine gene family, which is involved in numerous biological processes of diseases, such as tumor progression. Its upregulated expression is closely associated with the development of colorectal cancer. However, research on the role of GALNT12 in fibrosarcoma is currently limited. The present study aimed to assess the expression and biological function of GALNT12 in fibrosarcoma. Patient data and tissue samples were collected and public datasets were obtained from the Gene Expression Omnibus (GSE24369 and GSE21124). Immunofluorescence assays were performed to observe the cellular localization of GALNT12. GALNT12 expression was measured using reverse transcription-quantitative PCR, western blotting and immunohistochemistry. Small interfering RNAs were constructed to knock down GALNT12 expression in HT-1080 cells. Cell Counting Kit-8 and EdU assays were used to assess fibrosarcoma cell proliferation. Wound healing and Transwell assays were used to detect migration. Gene set enrichment analysis was performed to identify key pathways. Paired and unpaired Student's t-test, Fisher's exact test and one-way ANOVA (followed by Tukey's Honest Significant Difference test) were used to analyze the data. It was demonstrated that GALNT12 expression was upregulated in both fibrosarcoma cell lines and tissue samples and predicted poor patient prognosis. *In vitro* experiments demonstrated that high GALNT12 expression levels significantly increased HT-1080 cell proliferation and migration. Furthermore, it was demonstrated that high

GALNT12 expression levels were closely associated with the yes1 associated transcriptional regulator (YAP1) signaling pathway. Knockdown of GALNT12 inhibited YAP1 nuclear translocation, which affected activation of key downstream genes including AMOTL2, BIRC5 and CYR61. Therefore, the present study demonstrated that GALNT12 promoted fibrosarcoma progression. GALNT12 could be a potential biomarker for this disease and may potentially provide new ideas for targeted therapy of fibrosarcoma in the future.

Introduction

Soft tissue sarcoma is a type of tumor that originates from mesenchymal tissues (1). Soft tissue sarcoma accounts for ~0.7% of adult malignancies in the USA (2) and consists of >100 subtypes (3). According to the 4th edition of the World Health Organization Classification of Tumors of Soft Tissue and Bone, fibrosarcoma belongs to the subclass of fibroblastic or myofibroblastic tumors, representing ~3.6% of soft tissue sarcomas (4,5). Fibrosarcoma typically occurs in middle-aged and elderly patients, with a median age of onset of 50 years (6). It is commonly revealed that soft tissue sarcoma occurs in the trunk (13%), extremities (40-50%), and head and neck regions (9%) (7). The prognosis of patients with soft tissue sarcoma varies and is associated with both histopathological type and treatment response (7). Overall, soft tissue sarcoma has a poor prognosis, with a 5-year survival rate of <50% and a recurrence rate of >50% after surgery (8,9). Therefore, an in-depth understanding of the molecular mechanisms underlying fibrosarcoma pathogenesis could facilitate the development of novel targeted therapies for this malignant disease.

To date, researchers have identified ~18 members of the polypeptide N-acetylgalactosaminyltransferase (GALNT) gene family that serve important roles in tumor progression, lipid regulation, type 2 diabetes, neurodevelopmental disorders and various other diseases (10-13). As a member of the GALNT family, GALNT12 has two isoforms (Q8IXK2-1 and Q8IXK2-2) and is located on chromosome 9 (14). The GALNT12 protein has a molecular weight of ~66.9 kDa (14). GALNT12 encodes a glycosyltransferase that catalyzes the first step of mucin-type O-linked protein glycosylation, transferring N-acetylgalactosamine (GalNAc) from uridine diphosphate-GalNAc to serine or threonine residues on polypeptide acceptors (15). Abnormal GALNT12 expression has been reported in various diseases. For example, abnormal

Correspondence to: Professor Pihong Zhang, Department of Burns and Plastic Surgery, Xiangya Hospital, Central South University, 87 Xiangya Road, Changsha, Hunan 410008, P.R. China
E-mail: zphong2022@126.com

*Contributed equally

Key words: fibrosarcoma, polypeptide N-acetylgalactosaminyltransferase 12, yes1 associated transcriptional regulator, tumor growth

GALNT12 expression has been revealed in several autoimmune diseases including IgA nephropathy, rheumatoid arthritis and autoimmune inner ear disease (16-18). Previous studies have reported genetic variations or abnormal GALNT12 expression in tumors such as colorectal, glioblastoma, endometrial cancer and lymphoma, which is associated with their malignant phenotypes (19-23). However, to the best of our knowledge, GALNT12 expression has not been reported in fibrosarcoma and its expression pattern and impact on the malignant behavior of fibrosarcoma is currently unknown. Therefore, the present study aimed to investigate GALNT12 expression in fibrosarcoma and its influence on biological functions.

Materials and methods

Patients and tissue samples. In the present study, primary fibroblastic or myofibroblastic tumors from 22 patients that underwent surgical resection at Xiangya Hospital of Central South University (Changsha, China) from 01/01/2017-10/31/2022 were sampled. Patients were aged between 8 and 84 years, and there were 15 male patients and 7 female patients. After surgical resection, all specimens were immediately placed in tissue-protective solution (Biosharp), frozen in liquid nitrogen and stored at -80°C . Tissue samples were used to prepare sections for immunohistochemistry (IHC). Fibrosarcoma tissues from 6 of the 22 cases were also used for mRNA and protein extraction. Clinicopathological characteristics of enrolled patients were obtained from medical records. Tumors were classified histologically using guidelines published in the American Joint Committee on Cancer Limb/Torso Soft Tissue Sarcoma Staging System (8th edition, 2017) (24). The present study was approved by the Ethics Committee of Xiangya Hospital and written informed consent was obtained from all participants or their guardians (ethics approval no. 201603079).

Public datasets. Fibroblastic or myofibroblastic tumor datasets (GSE24369 and GSE21124, respectively) were selected from the Gene Expression Omnibus (GEO) database for gene selection (control group, $n=6$; tumor group, $n=6$; from different patients) and GSE21124 (control group, $n=9$; tumor group, $n=34$; from different patients).

Cell culture. Human fibrosarcoma HT-1080 cells and human skin fibroblasts (HSF; HSA-S4) were purchased from Abiowell (Changsha Abiowell Biotechnology Co., Ltd.) with STR certification reports. Cells were cultured in high-glucose DMEM (Gibco; Thermo Fisher Scientific, Inc.) supplemented with 10% fetal bovine serum (FBS; Shanghai ExCell Biology, Inc.) and 1% penicillin/streptomycin at 37°C with 5% CO_2 .

IHC. IHC was performed as previously described (25). Staining intensity and percentage of positivity were analyzed by ImageJ/Fiji (2.15.0; Github; <https://imagej.net/software/fiji/>) (26). Staining was evaluated and graded by two independent investigators. The staining intensity scoring was 0 (negative), 1 (weak), 2 (moderate) and 3 (strong). The degree of staining was stratified as 0 (0%), 1 (1-25%), 2 (26-50%), 3 (51-75%) and 4 (76-100%), and was defined as the percentage of positive staining area in the total tumor invasion area.

The final score of GALNT12 expression was determined by adding the intensity of staining to the degree of staining; its value was 0-7. The samples were divided into two groups: Low GALNT12 expression (0-3 points) and high GALNT12 expression (4-7 points). Sections were classified into high and low expression groups. The primary antibody used was: Anti-GALNT12 (1:100; cat. no. K108365P; Beijing Solarbio Science & Technology Co., Ltd.). A HRP-conjugated antibody (1:200; cat. no. GB23303; Wuhan Servicebio Technology Co., Ltd. 1:200 for IHC) was used as a secondary antibody.

Immunocytochemistry. Immunocytochemistry was performed as previously described (25). The primary antibody used was: Anti-GALNT12 (1:50; cat. no. K108365P; Beijing Solarbio Science & Technology Co., Ltd.). CoraLite594-conjugated Goat Anti-Rabbit IgG (H+L) (1:200; cat. no. SA00013-4; Proteintech Group, Inc.) was used as a secondary antibody.

RNA extraction and reverse transcription-quantitative PCR (RT-qPCR). Total RNA of fibrosarcoma tissues or HT-1080 cells was extracted using *TransZol Up* (TransGen Biotech Co., Ltd.) according to the manufacturer's instructions. The quality and concentration of the isolated RNA were analyzed using a NanoDrop 2000 (Thermo Fisher Scientific, Inc.) and reverse transcribed into cDNA using the Evo M-MLV RT kit (Accurate Biology) according to the manufacturer's instructions. RT-qPCR was performed on the Vii7 system (Applied Biosystems; Thermo Fisher Scientific, Inc.) using ribosomal protein S18 (RPS18) as an internal normalization control. Relative mRNA expression was calculated using the $2^{-\Delta\Delta\text{C}_q}$ method (27). Primer sequences are listed in Table S1. For qPCR, 2X SYBR Green qPCR Master Mix (Low ROX) (cat. no. G3321-15; Wuhan Servicebio Technology Co., Ltd.) was used. The recommended qPCR procedure was as follows: Stage 1, 95°C for 30 sec for one cycle; stage 2, 95°C for 15 sec and 60°C for 30 sec for 40 cycles; stage 3, 95°C for 15 sec, 60°C for 60 sec and 95°C for 15 sec for one cycle.

Western blotting. HSF cells, HT-1080 cells and fibrosarcoma tissues were lysed in RIPA buffer (Beyotime Institute of Biotechnology) with protease inhibitors (Wuhan Servicebio Technology Co., Ltd.) (RIPA buffer:protease inhibitors, 100:1) for 15 min on ice to extract total proteins. The BCA method was used to determine protein concentrations. Subsequently, proteins were boiled with 5X loading buffer (Wuhan Servicebio Technology Co., Ltd.) for 10 min. Nuclear proteins were isolated using a commercial kit (cat. no. R0050; Beijing Solarbio Science & Technology Co., Ltd.) following the manufacturer's protocol. Proteins (50 $\mu\text{g}/\text{lane}$) were separated using a 10% gel with SDS-PAGE and transferred to PVDF membranes. Membranes were blocked with 5% BSA (BioFroxx; neoFroxx GmbH) or 5% milk (BD Biosciences) in TBS for 1 h at room temperature before incubating with primary antibodies (overnight at 4°C) and secondary antibodies (1 h at room temperature). 5% BSA was used to block membranes to assess p-YAP1; 5% milk was used to block membranes to assess other molecules (GALNT12, GAPDH, YAP1 and Lamin B1). The primary antibodies used were: GALNT12 (cat. no. K108365P; Beijing Solarbio Science & Technology Co., Ltd.), GAPDH (cat. no. GB15004; Wuhan Servicebio

Technology Co., Ltd.), yes1 associated transcriptional regulator (YAP1; cat. no. ET1608-30; HUABIO), phosphorylated (p)-YAP1 (cat. no. ET1611-69; HUABIO) and Lamin B1 (cat. no. ET1606-27; HUABIO). The HRP-conjugated secondary antibodies (cat. no. GB23303; Wuhan Servicebio Technology Co., Ltd.) were used. Protein bands were visualized using ECL reagent (Wuhan Servicebio Technology Co., Ltd.) in ChemiDoc™ (BioRad Laboratories, Inc.). ImageJ/Fiji (2.15.0; Github) was used to measure the bands densitometry.

Nuclear protein extraction. Nuclear proteins were extracted using the Nuclear Protein Extraction kit (cat. no. R0050; Beijing Solarbio Science & Technology Co., Ltd.) according to the manufacturer's protocols. Cells were washed with 1x PBS, and then cytoplasmic protein extraction reagent was added and the mixture was incubated on ice for 10 min. Cells were centrifuged (12,000 x g for 10 min at 4°C) and the supernatant was collected to obtain cytoplasmic proteins. Subsequently, nuclear protein extraction reagent was added to the remaining cell sediment. This mixture was incubated on ice for 10 min, and then the supernatant was collected after centrifugation (12,000 x g for 10 min at 4°C) to obtain nuclear proteins.

Small interfering (si)RNA knockdown. HT-1080 cells (5×10^5) were seeded in 6-well plates before transfection. At 70% confluence, cells were transfected with 100 pmol siRNA against GALNT12 (siGALNT12-1 and siGALNT12-2) or non-targeting control siRNA (Table SII; TsingKe Biological Technology) using Lipo6000 (Beyotime Institute of Biotechnology) in Opti-MEM (Gibco; Thermo Fisher Scientific, Inc.). After 8 h at 37°C, high-glucose DMEM supplemented with 10% fetal bovine serum (Shanghai ExCell Biology, Inc.) was added. After 48 h, transfected cells were used for further experiments.

Cell Counting Kit-8 (CCK-8) assay. Cell viability was assessed using a CCK-8 assay. HT-1080 cells were seeded in 96-well plates (2×10^3 cells/well) and transfected with GALNT12 siRNAs and negative control siRNAs. After transfection, 10 μ l CCK-8 reagent (Beyotime Institute of Biotechnology) was added to each well and incubated for 2 h in the dark. Absorbance at 450 nm was measured using a SpectrumMax Plus384 microplate reader (Molecular Devices, LLC).

EdU assay. HT-1080 cells (2×10^5 cells per well) were seeded in 6-well plates and allowed to adhere at 37°C for 24 h. Cells were incubated with EdU reagent (Wuhan Servicebio Technology Co., Ltd.), fixed with 4% paraformaldehyde, permeabilized with Triton X-100 and stained following the manufacturer's protocol. Nuclei were counterstained with 5 μ g/ml Hoechst 33342 (Wuhan Servicebio Technology Co., Ltd.) for 15 min at room temperature. Cells were imaged using a Nikon inverted fluorescence microscope (Nikon ECLIPSE Ti2; Nikon Corporation).

Wound healing assay. HT-1080 cells were seeded in 6-well plates (3×10^5 cells/well) and grown to 100% confluence. A sterile pipette tip was used to create vertical scratches across the cell monolayer and the cells were then cultured with fresh serum-free medium at 37°C. Images were captured at 0 and

24 h post-scratch using a Nikon inverted light microscope (Nikon ECLIPSE Ti2). Cell migration distance was judged by comparing the distance between the initial scratch (0 h) and the scratch at the 24-h observation point, which was measured using ImageJ/Fiji software (2.15.0; Github).

Transwell assay. Transwell chambers (pore size, 8 μ m; Corning, Inc.) were prepared with 500 μ l serum-free DMEM in the upper chamber and 3×10^5 HT-1080 cells/well. The lower chamber contained 500 μ l DMEM with 20% FBS. After culturing at 37°C for 24 h, cells were fixed in 4% paraformaldehyde for 15 min, stained with 0.1% crystal violet for 10 min at room temperature, imaged under a light microscope (Nikon ECLIPSE Ti2) and counted.

Gene set enrichment analysis (GSEA). GSEA (version 4.2.3, <https://www.gsea-msigdb.org/gsea/index.jsp>) was performed on the GSE2553 dataset to identify key enriched pathways. Normalized Enrichment Score (NES), P-value and false discovery rate (FDR) are the main observables for enrichment analysis (cut off values: NES >1, P<0.05, FDR <0.25).

Statistical analysis. GraphPad Prism (version 9.0; Dotmatics) was used for data analysis. Paired and unpaired Student's t-test, Fisher's exact test and one-way ANOVA (followed by Turkey's Honest Significant Difference test) were used to analyze statistical differences between groups. P<0.05 was considered to indicate a statistically significance difference.

Results

GALNT12 is upregulated in fibroblastic and myofibroblastic tumors. To explore gene expression level changes in fibrosarcoma, the GSE24369 and GSE21124 public datasets from GEO were analyzed. A total of 308 and 578 differentially expressed genes (DEGs) in GSE24369 and GSE21124 were identified, respectively (P<0.05; log₂ fold change >1.5). Comparisons between these datasets identified 15 common DEGs (Fig. 1A). Among these, fatty acid binding protein 3, GALNT12, protein regulator of cytokinesis 1 and CDC28 protein kinase regulatory subunit 2 were highly expressed in tumors (Fig. 1B). Based on the statistical significance observed and the previous literature (19-23), GALNT12 was selected for further analysis. GALNT12 mRNA levels were significantly increased in the tumor groups in both datasets when compared with the control group (P<0.01; Fig. 1C). In the GSE21124 dataset, GALNT12 demonstrated significantly increased expression among GALNT family members GALNT7, GALNT10 and GALNT12 when compared with the control group (P<0.01; Fig. 1D). Immunofluorescent analysis demonstrated cytoplasmic localization of the GALNT12 protein in HT-1080 cells (Fig. 1E).

GALNT12 expression is upregulated in fibrosarcoma. Analysis of both public and acquired patient data demonstrated increased GALNT12 mRNA and protein expression levels in fibrosarcoma. In the GSE2719 GEO dataset, GALNT12 mRNA expression levels were increased in tumor tissues compared with normal tissues (P<0.05; Fig. 2A). RT-qPCR results also demonstrated increased GALNT12 mRNA expression levels

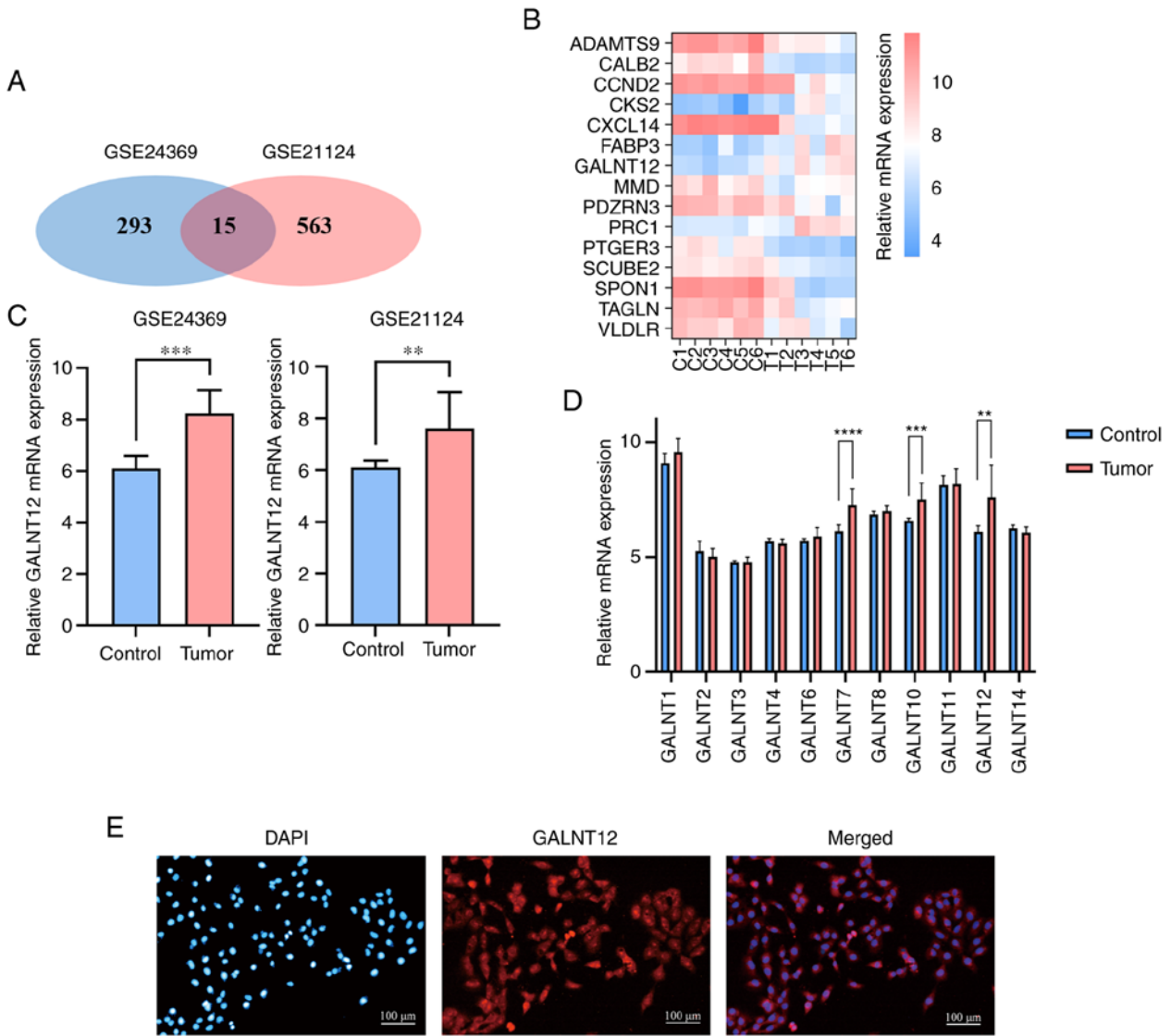


Figure 1. Analysis of publicly available fibroblast and myofibroblast datasets. (A) Intersection of DEGs in GSE24369 and GSE21124 datasets. (B) Relative mRNA expression of 15 DEGs in the heatmap (DEGs: $P < 0.05$ and \log_2 fold change > 1.5). (C) Relative mRNA expression of GALNT12 in GSE24369 (control group, $n=6$; tumor group, $n=6$; from different patients) and GSE21124 (control group, $n=9$; tumor group, $n=34$) datasets. Unpaired Student's t-tests were used to analyze the difference between control and tumor groups. (D) Relative mRNA expression of GALNT family members in the GSE21124 dataset. Unpaired Student's t-tests were used to analyze the difference between control and tumor groups. (E) Cytofluorimetric localization of the GALNT12 protein in HT-1080 cells. Scale bar, 100 μm . Data were presented as the mean \pm standard deviation. ** $P < 0.01$; *** $P < 0.001$; **** $P < 0.0001$. DEGs, differentially expressed genes; GALNT12, polypeptide N-acetylgalactosaminyltransferase 12; C, control; T, tumor.

in HT-1080 cells compared with normal fibroblasts ($P < 0.05$; Fig. 2B). Immunoblotting demonstrated increased GALNT12 protein expression levels in six fibrosarcoma samples compared with healthy tissue controls (Fig. 2C).

High GALNT12 expression levels are associated with poor prognosis in patients with fibrosarcoma. IHC staining demonstrated an increased expression of GALNT12 in fibrosarcoma tissues compared with adjacent healthy tissue (Fig. 3A and B). High GALNT12 expression was significantly associated with larger tumor size ($P = 0.002$) and advanced T-stage ($P = 0.027$) (Table I).

GALNT12 knockdown suppresses proliferation of HT-1080 cells. The present study investigated the impact of GALNT12 on the biological behavior of fibrosarcoma cells. siRNAs targeting GALNT12 were used to knock down GALNT12

expression levels in HT-1080 cells. The efficiency of transfection was confirmed with RT-qPCR analysis (Fig. 4A). Subsequently, the CCK-8 assay demonstrated reduced cell viability in the GALNT12 knockdown groups compared with the negative control group (Fig. 4B). Moreover, the EdU assay demonstrated a significant decrease in cell proliferation in the GALNT12 knockdown groups compared with the negative control ($P < 0.05$; Fig. 4C and D).

GALNT12 knockdown impairs migration of HT-1080 cells. To assess the influence of GALNT12 on cell motility, both wound healing and Transwell assays were used with transfected HT-1080 cells. The Transwell assay demonstrated a significant reduction in the number of cells traversing the chamber in the GALNT12 knockdown groups compared with the control group ($P < 0.0001$; Fig. 5A and B). Additionally, the

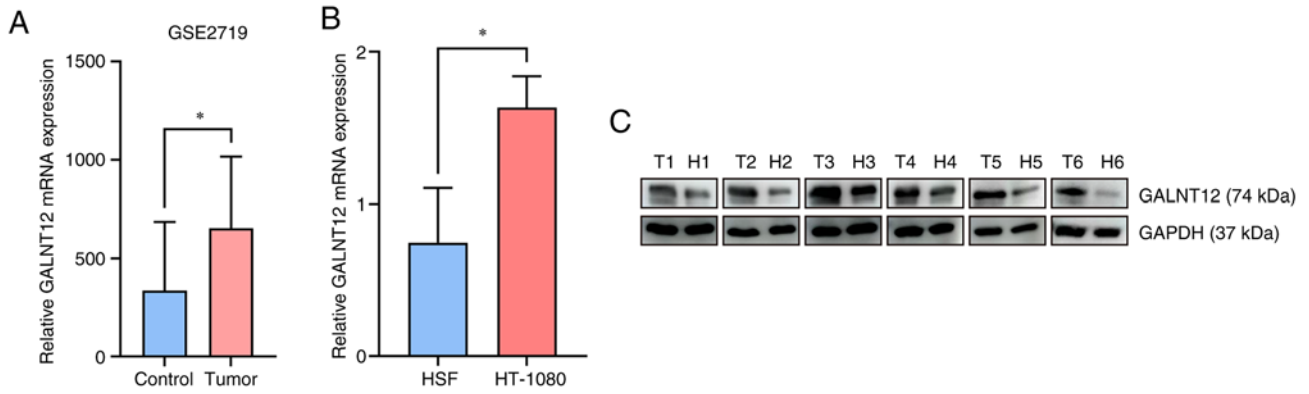


Figure 2. Expression levels of GALNT12. Relative mRNA expression levels of GALNT12 in (A) GSE2719 (control group, n=15; tumor group, n=9) and (B) GALNT12 in HSF and HT-1080 cells (n=3/group). Unpaired Student's t-tests were used to analyze the differences between the two groups. (C) Relative protein expression levels of GALNT12 in fibrosarcoma tissues and healthy control tissues. Data were presented as the mean ± standard deviation (n=3). *P<0.05. HSF, human skin fibroblasts; GALNT12, polypeptide N-acetylgalactosaminyltransferase 12; T, tumor; H, healthy tissue.

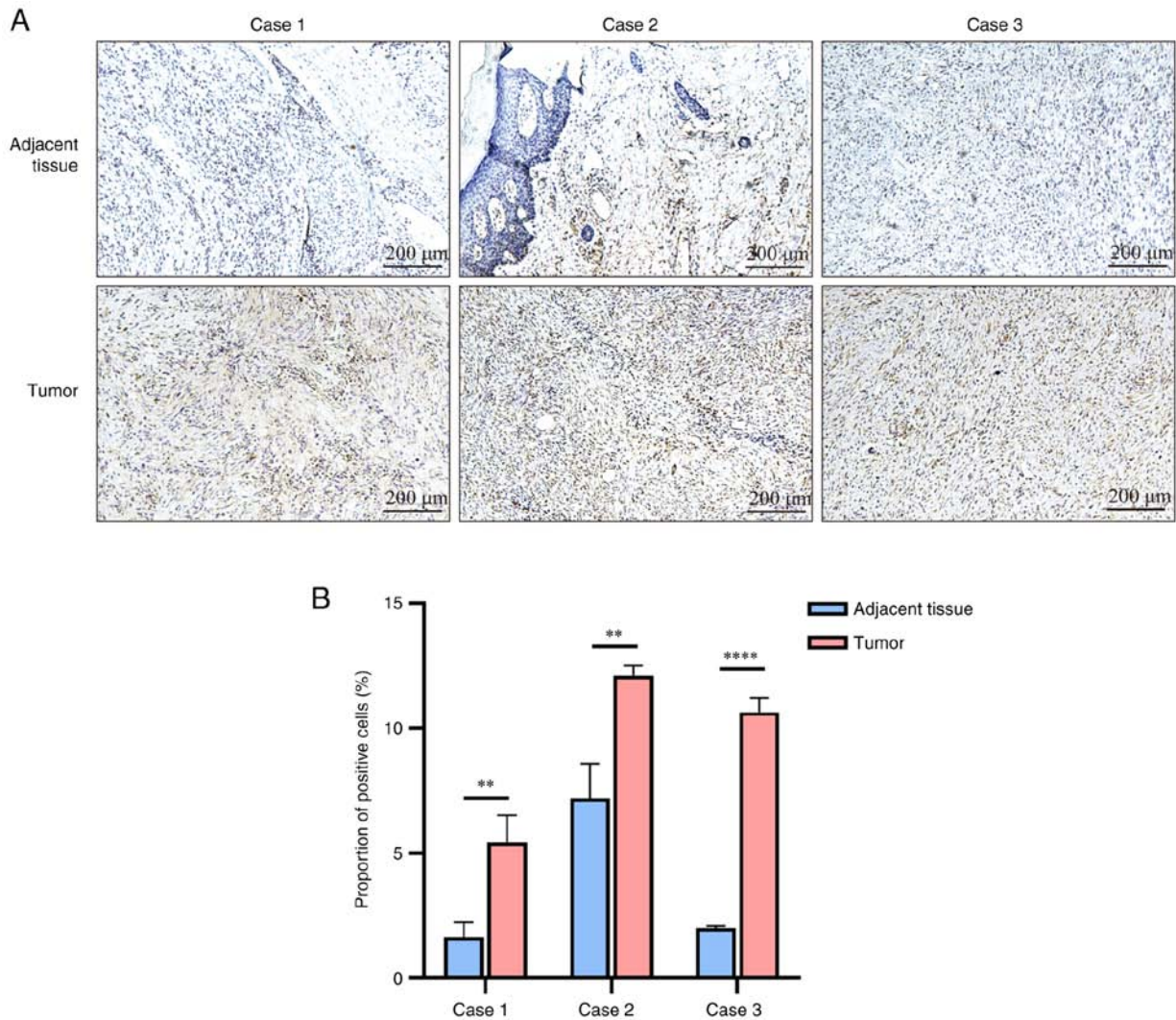


Figure 3. Expression of GALNT12 in fibrosarcoma. (A) IHC staining of GALNT12 in 3 fibrosarcoma tissues (scale bar, 200 μm) and (B) proportion of GALNT12-positive cells. Each experiment was performed three times and measurement data were presented as the mean ± standard deviation. **P<0.01; ****P<0.0001. GALNT12, polypeptide N-acetylgalactosaminyltransferase 12.

wound healing assay demonstrated a reduced migration in the GALNT12 knockdown groups compared with the control group (P<0.01; Fig. 5C and D).

GALNT12 enhances tumor malignancy by facilitating YAP1 nuclear localization. Using the GSE2553 dataset from the GEO database, samples were categorized into high and low

Table I. Relationship between GALNT12 expression and clinical factors.

| Patient characteristic | Number of patients (n) | Low GALNT12 expression (n) | High GALNT12 expression (n) | P-value |
|---------------------------------|------------------------|----------------------------|-----------------------------|---------|
| Age, years | | | | |
| ≤35 | 11 | 7 | 4 | 0.080 |
| >35 | 11 | 2 | 9 | |
| Sex | | | | |
| Male | 15 | 5 | 10 | 0.376 |
| Female | 7 | 4 | 3 | |
| Tumor size, cm ³ | | | | |
| ≤43 | 10 | 8 | 2 | 0.002 |
| >43 | 12 | 1 | 11 | |
| Surrounding invasion of tissues | | | | |
| Yes | 10 | 4 | 6 | >0.999. |
| No | 12 | 5 | 7 | |
| Tumor stage | | | | |
| T1 | 9 | 7 | 2 | 0.027 |
| T2 | 7 | 1 | 6 | |
| T3 | 5 | 1 | 4 | |
| T4 | 1 | 0 | 1 | |
| Node stage | | | | |
| N0 | 20 | 8 | 12 | >0.999. |
| N1 | 2 | 1 | 1 | |
| Metastasis stage | | | | |
| M0 | 18 | 8 | 10 | 0.616 |
| M1 | 4 | 1 | 3 | |

T, tumor; N, node; M, metastasis; GALNT12, polypeptide N-acetylgalactosaminyltransferase 12.

GALNT12 mRNA expression groups. Through GSEA, the YAP1 signaling pathway was identified as pivotal in fibrosarcoma pathogenesis (Fig. 6A). Following GALNT12 knockdown, the phosphorylation level of YAP1 increased compared with the negative control group (Fig. 6B). The nuclear protein extraction assay demonstrated reduced YAP1 nuclear localization in the siGALNT12-1 and siGALNT12-2 groups compared with the negative control (Fig. 6C and D). Furthermore, RT-qPCR analysis demonstrated a significantly decreased expression of YAP1 downstream target genes, including CYR61, AMOTL2 and BIRC5, compared with the corresponding negative control groups ($P < 0.05$) (Fig. 6E). Based on these findings, it could be suggested that GALNT12 modulates the proliferation and migration capabilities of the fibrosarcoma cell line HT-1080 by influencing YAP1 nuclear localization (Fig. 7).

Discussion

Overcoming the challenges posed by therapeutic inefficacy and the elusive molecular mechanisms in fibrosarcoma remains a significant hurdle. Identifying effective therapeutic targets for this condition remains paramount. GALNT has emerged as an important component in the development

of human tumors, exerting influence over a spectrum of biological processes encompassing proliferation, invasion, apoptosis, angiogenesis and the epithelial-mesenchymal transition (EMT) of tumor cells (28-31). For example, GALNT2 has been implicated in enhancing migration and proliferation of colorectal cancer cells via AXL signaling (32). A previous study reported that GALNT3 suppressed lung cancer by inhibiting myeloid-derived suppressor cell infiltration and angiogenesis via a TNFR and c-MET pathway-dependent manner (33). Additionally, in trophoblast stem cells, blastocyst trophectoderm and human mammary epithelial cells, GALNT3 O-GalNAc glycosylation could promote the epithelial phenotype and the upregulation of GALNT3 expression is associated with the EMT (34). In various types of digestive system malignancies, including hepatocellular carcinoma, gastric cancer and esophageal cancer, increased GALNT14 expression is associated with accelerated tumor growth, reduced chemotherapy responsiveness and poor patient prognoses (35). Additionally, upregulation of GALNT7 in prostate cancer induces O-glycosylation alterations, which ultimately promotes tumor growth (36). GALNT5 and VVL-binding glycans have been identified as drivers of cholangiocarcinoma metastasis through the AKT/ERK signaling pathway (37). Furthermore, GALNT12 variants are associated with

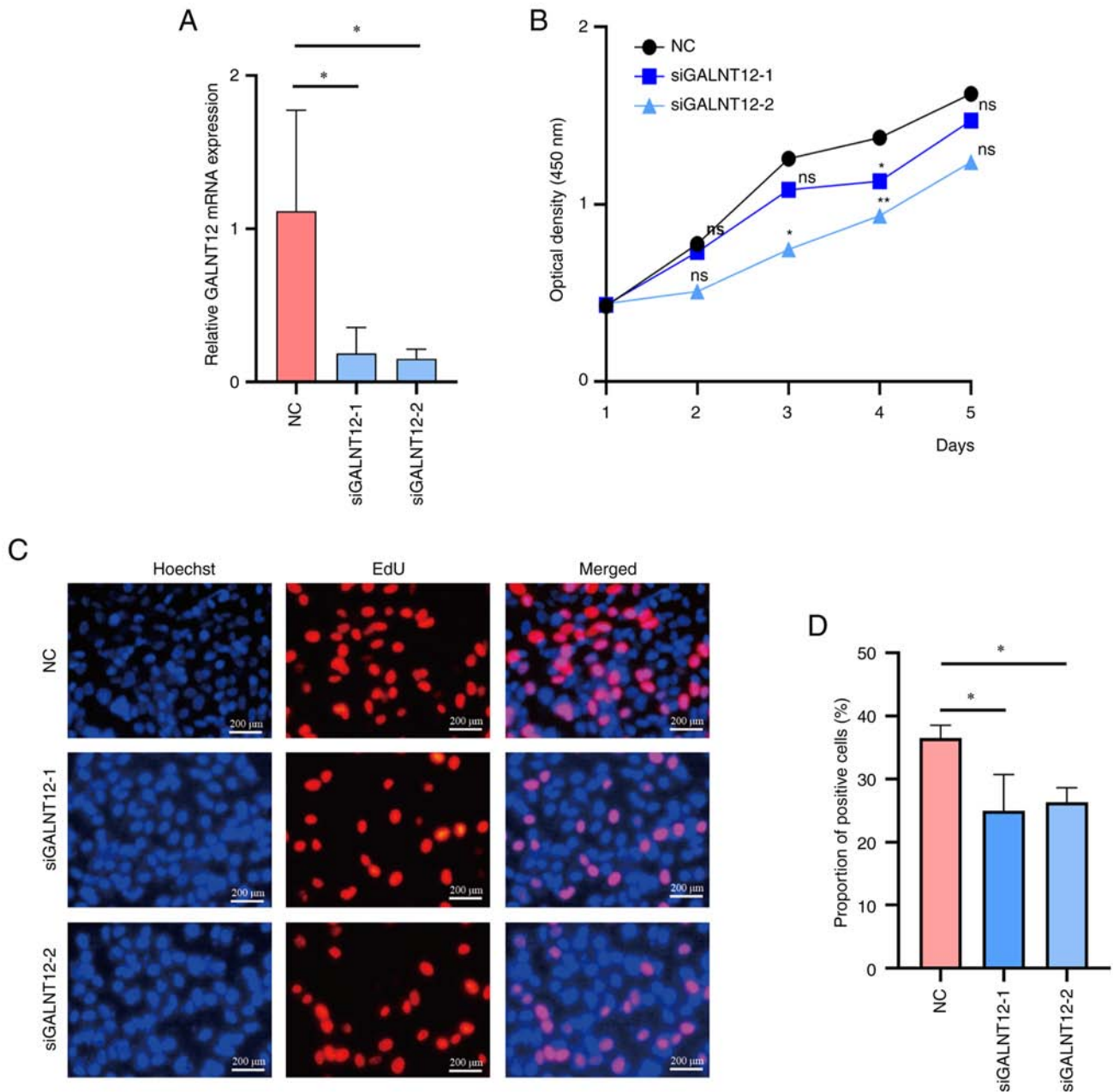


Figure 4. Knockdown of GALNT12 in HT-1080 cells suppresses proliferation. (A) Knockdown efficiency of GALNT12 in HT-1080 cells transfected with siRNA. (B) Cell viability of HT-1080 cells was measured using Cell Counting Kit-8 assays. Cell viability of HT-1080 cells was measured using (C) EdU assays (scale bar, 200 μ m) and (D) the proportion of viable cells was measured. One-way ANOVA (followed by Tukey's Honest Significant Difference test) was used to analyze differences between the three groups. Data were presented as the mean \pm standard deviation (n=3). *P<0.05; **P<0.01. GALNT12, polypeptide N-acetylgalactosaminyltransferase 12; NC, negative control; ns, not significant; si, small interfering.

increased susceptibility to colorectal cancer, demonstrating the significance of glycosylation pathway aberrations in this disease (20). GALNT12 has been reported to increase proliferation, invasion and metastasis of glioma cells via activation of the PI3K/AKT/mTOR signaling pathway (21). Moreover, Daseg *et al* (38) suggested that patched 1, ephrin type-B receptor 2, Ret proto-oncogene and GALNT12 may contribute to the synergistic oncogene-driven malignant transformation in ulcerating basal cell carcinomas. GALNT3 inhibits tumor cell growth in lung cancer or promotes the epithelial phenotype, whereas the majority of other GALNT family members promote tumor progression (20,21,34-38). This may be associated with their different molecular

structures and the tumor type. These previous studies collectively suggest that the GALNT family of proteins may serve an important role in tumor genesis, influencing key downstream signaling pathways that culminate in a malignant phenotype (20,21,34-38). In the present study, these findings were corroborated and it was demonstrated that an upregulation of GALNT12 occurred in human fibrosarcoma tissues and the HT-1080 cell line. Notably, the increased expression of GALNT12 was associated with tumor size and T-stage, indicating a poor prognosis for patients. *In vitro* assays further demonstrated a reduction in HT-1080 proliferation and migration in the GALNT12 knockdown groups compared with the controls. This collective evidence supported the

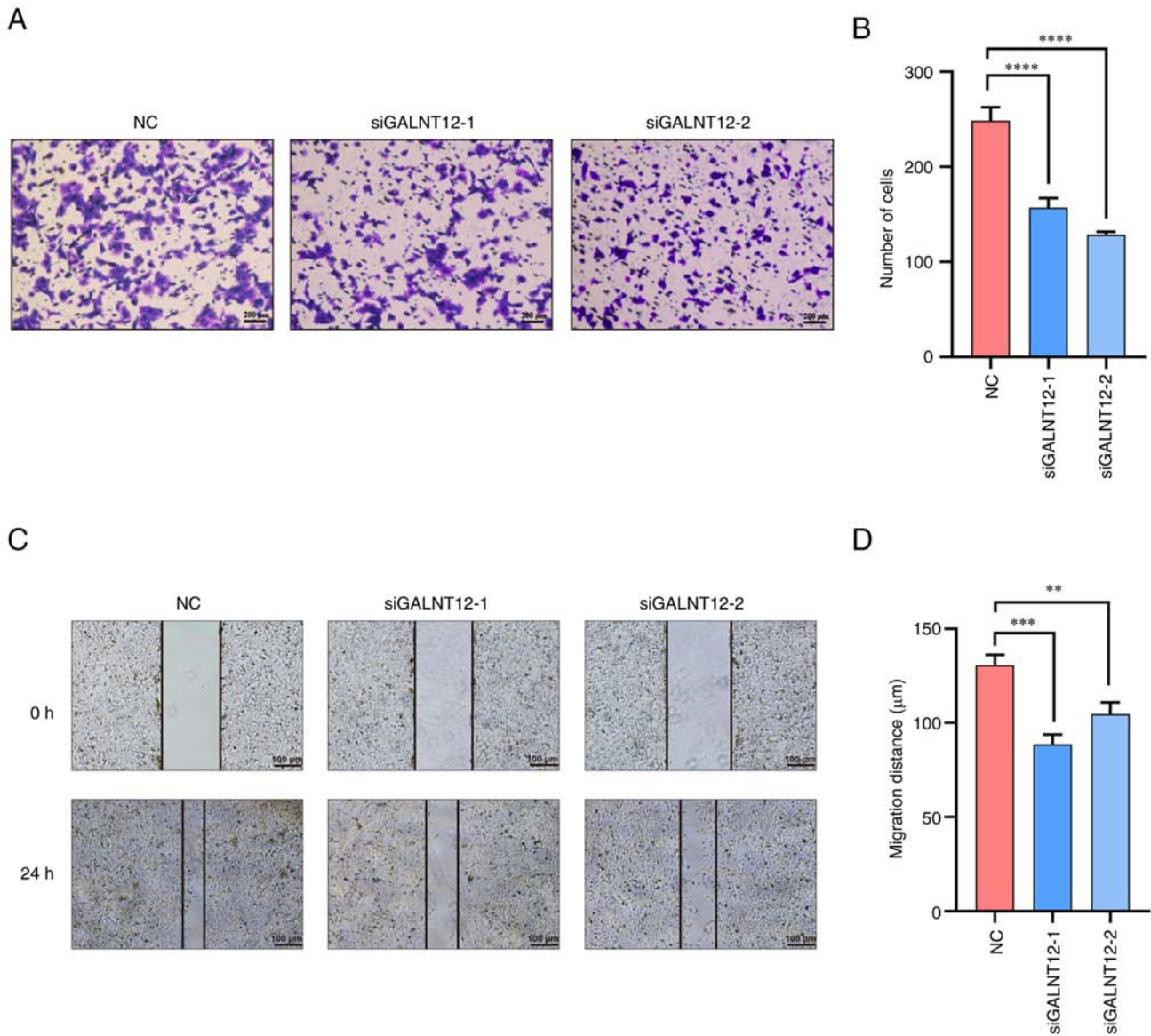


Figure 5. GALNT12 knockdown impairs migratory capacities of HT-1080 cells. Migration of HT-1080 cells was measured using (A) Transwell assays (scale bar, 200 μm) and (B) the results quantified. The migration ability of HT-1080 cells was measured using (C) wound healing assays (scale bar, 100 μm) and (D) the results quantified. One-way ANOVA (followed by Tukey's Honest Significant Difference test) was used to analyze the differences between the three groups. Data were presented as the mean \pm standard deviation ($n=3$). ** $P<0.01$; *** $P<0.001$; **** $P<0.0001$. si, small interfering; GALNT12, polypeptide N-acetylgalactosaminyltransferase 12; NC, negative control.

hypothesis that GALNT12 could be a potential therapeutic target for fibrosarcoma. However, due to the diverse array of tumor types, distinct expression patterns within each tumor and molecular disparities among GALNT family members, GALNT proteins likely use varying molecular mechanisms to drive tumor progression. Therefore, further research is required to unravel the molecular intricacies underpinning fibrosarcoma progression.

The activation of the YAP1 signaling pathway has previously been implicated to foster malignant behaviors such as cell proliferation, invasion, EMT and metastasis (39-41). For example, Liu *et al* (42) elucidated the role of the signaling axis ZIP4-miR-373-LATS2-ZEB1/YAP1-ITGA3 in pancreatic cancer metastasis and EMT plasticity. Ajani *et al* (43) reported a significant upregulation of YAP1 in peritoneal carcinomatosis tumor cells, which conferred cancer stem cell

properties and potentially promoted metastasis. Additionally, in the present study, GSEA demonstrated that dysregulation of GALNT12 affected the downstream YAP1 signaling pathway. Knockdown of GALNT12 significantly reduced the nuclear localization of YAP1, which consequently suppressed the activation of downstream target genes and impeded tumor cell growth. Thus, it could be suggested that GALNT12 promoted the growth of the fibrosarcoma cell line HT-1080 through facilitation of YAP1 nuclear localization. Further elucidation of the YAP1 signaling pathway could hold promise for unravelling the molecular underpinnings of fibrosarcoma.

In summary, the present study highlighted the increased expression levels of GALNT12 in clinical tumor tissues, which was associated with worsened patient prognoses. Through *in vitro* assays, the pro-carcinogenic role of

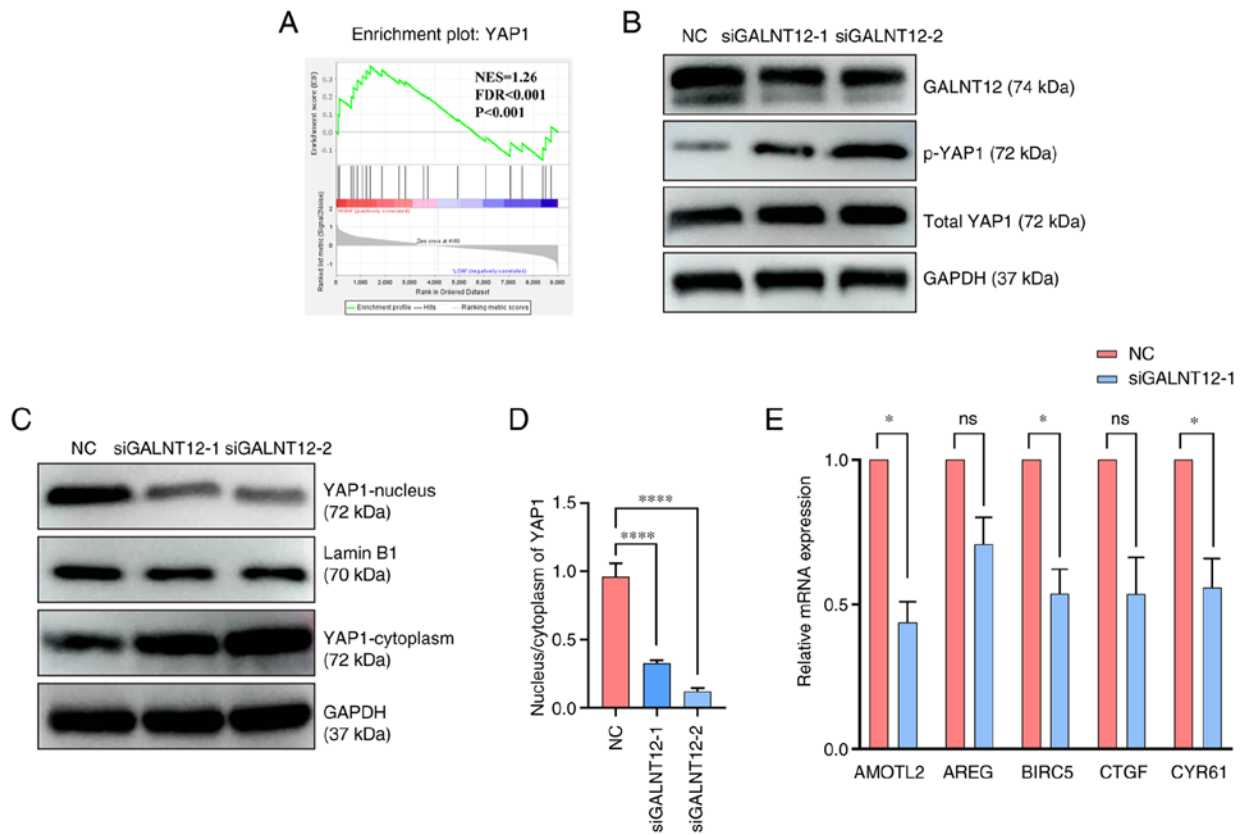


Figure 6. GALNT12 enhances malignancy by facilitating YAP1 nuclear localization. (A) Gene Set Enrichment Analysis was performed on the GSE2553 dataset. (B) Protein expression levels of GALNT12, YAP1, p-YAP1 and GAPDH were measured in transfected HT-1080 cells using western blotting. (C) Protein expression levels of YAP1 in the nucleus and cytoplasm of cells were measured and (D) the ratio of localization was quantified. One-way ANOVA (followed by Tukey's Honest Significant Difference test) was used to analyze the differences between the three groups. (E) Relative mRNA levels of AMOTL2, AREG, BIRC5, CTGF and CYR61 were detected using reverse transcription-quantitative PCR. siGALNT12-1 was used for this assay to interfere with the expression of GALNT12. Unpaired Student's t-tests were used to analyze the differences between the two groups. Data were presented as the mean ± standard deviation (n=3). *P<0.05; ****P<0.001. ns, not significant; si, small interfering; NC, negative control; GALNT12, polypeptide N-acetylgalactosaminyltransferase 12; YAP1, yes1 associated transcriptional regulator; p, phosphorylated; CYR61, cysteine-rich angiogenic inducer 61; CTGF, connective tissue growth factor; AREG, amphiregulin; AMOTL2, angiomin-like 2; BIRC5, baculoviral IAP repeat containing 5; NES, normalized enrichment score; FDR, false discovery rate.

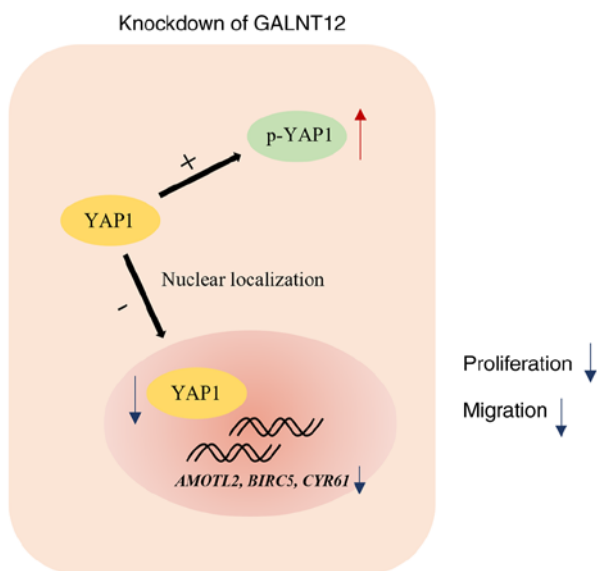


Figure 7. Schematic diagram of GALNT12 regulating YAP1 nuclear localization. YAP1, yes1 associated transcriptional regulator; p, phosphorylated; GALNT12, polypeptide N-acetylgalactosaminyltransferase 12; AMOTL2, angiomin-like 2; BIRC5, baculoviral IAP repeat containing 5; CYR61, cysteine-rich angiogenic inducer 61.

GALNT12 in the fibrosarcoma cell line HT-1080 was investigated, including analyzing the cell viability, proliferation and migration potential of these cells. The present study demonstrated GALNT12 as an important oncogenic protein in fibrosarcoma, and offered fresh perspectives and potential future avenues for targeted therapeutic interventions to treat this disease.

Acknowledgements

Not applicable.

Funding

This study received support from the Academic Construction Funding of Xiangya Hospital, Central South University (grant no. XK60000691391).

Availability of data and materials

The datasets used and/or analyzed during the current study are available from the corresponding author on reasonable request.

Authors' contributions

PZ and SY conceptualized the study. WF, JZ, SZ and YP contributed to specimen collection. SY and WF conducted the experiments. SY performed data analysis and drafted the manuscript. SY and WF confirm the authenticity of all the raw data. All authors read and approved the final version of the manuscript.

Ethics approval and consent to participate

Informed written consent was obtained from all patients. The study was conducted in accordance with the Declaration of Helsinki and approved by the Ethics Committee of Xiangya Hospital, Central South University (ethics approval no. 201603079).

Patient consent for publication

Not applicable.

Competing interests

The authors declare that they have no competing interests.

References

- Pankova V, Thway K, Jones RL and Huang PH: The extracellular matrix in soft tissue sarcomas: Pathobiology and cellular signaling. *Front Cell Dev Biol* 9: 763640, 2021.
- American Cancer Society. What is a soft tissue sarcoma? American Cancer Society, Atlanta, GA, 2023. <https://cancerstatisticscenter.cancer.org/#/>.
- Howlander N, Noone AM, Krapcho M, Miller D, Brest A, Yu M, Ruhl J, Tatalovich Z, Mariotto A, Lewis DR, *et al* (eds): SEER cancer statistics review, 1975-2018. National Cancer Institute, Bethesda, MD, 2020.
- Fletcher CDM, Bridge JA, Hogendoorn PCW and Mertens F (eds): WHO classification of tumours of soft tissue and bone. In: WHO Classification of Tumours. 4th edition. Vol. 5. IARC Press, Lyon, 2013.
- Toro JR, Travis LB, Wu HJ, Zhu K, Fletcher CDM and Devesa SS: Incidence patterns of soft tissue sarcomas, regardless of primary site, in the surveillance, epidemiology and end results program, 1978-2001: An analysis of 26,758 cases. *Int J Cancer* 119: 2922-2930, 2006.
- Bahrami A and Folpe AL: Adult-type fibrosarcoma: A reevaluation of 163 putative cases diagnosed at a single institution over a 48-year period. *Am J Surg Pathol* 34: 1504-1513, 2010.
- Gamboia AC, Gronchi A and Cardona K: Soft-tissue sarcoma in adults: An update on the current state of histiotype-specific management in an era of personalized medicine. *CA Cancer J Clin* 70: 200-229, 2020.
- Francis M, Charman J, Dennis N, Lawrence G and Grimer R: Bone and soft tissue sarcomas. UK Incidence and Survival: 1996 to 2010. Version 2.0. National Cancer Intelligence Network, Bethesda, MD, 2013.
- Folpe AL: Fibrosarcoma: A review and update. *Histopathology* 64: 12-25, 2014.
- Phelan CM, Tsai YY, Goode EL, Vierkant RA, Fridley BL, Beesley J, Chen XQ, Webb PM, Chanock S, Cramer DW, *et al*: Polymorphism in the GALNT1 gene and epithelial ovarian cancer in non-Hispanic white women: The ovarian cancer association consortium. *Cancer Epidemiol Biomarkers Prev* 19: 600-604, 2010.
- Khetarpal SA, Schjoldager KT, Christoffersen C, Raghavan A, Edmondson AC, Reutter HM, Ahmed B, Ouazzani R, Peloso GM, Vitali C, *et al*: Loss of function of GALNT2 lowers high-density lipoproteins in humans, nonhuman primates, and rodents. *Cell Metab* 24: 234-245, 2016.
- Marucci A, di Mauro L, Menzaghi C, Prudente S, Mangiacotti D, Fini G, Lotti G, Trischitta V and Di Paola R: GALNT2 expression is reduced in patients with Type 2 diabetes: Possible role of hyperglycemia. *PLoS One* 8: e70159, 2013.
- Reuter MS, Tawamie H, Buchert R, Hosny Gebril O, Froukh T, Thiel C, Uebe S, Ekici AB, Krumbiegel M, Zweier C, *et al*: Diagnostic yield and novel candidate genes by exome sequencing in 152 consanguineous families with neurodevelopmental disorders. *JAMA Psychiatry* 74: 293-299, 2017.
- Guo JM, Zhang Y, Cheng L, Iwasaki H, Wang H, Kubota T, Tachibana K and Narimatsu H: Molecular cloning and characterization of a novel member of the UDP-GalNAc:polypeptide N-acetylgalactosaminyltransferase family, pp-GalNAc-T12. *FEBS Lett* 524: 211-218, 2002.
- Fernandez AJ, Daniel EJP, Mahajan SP, Gray JJ, Gerken TA, Tabak LA and Samara NL: The structure of the colorectal cancer-associated enzyme GalNAc-T12 reveals how nonconserved residues dictate its function. *Proc Natl Acad Sci USA* 116: 20404-20410, 2015.
- Wang YN, Zhou XJ, Chen P, Yu GZ, Zhang X, Hou P, Liu LJ, Shi SF, Lv JC and Zhang H: Interaction between GALNT12 and CIGALT1 associates with galactose-deficient IgA1 and IgA nephropathy. *J Am Soc Nephrol* 32: 545-552, 2021.
- Hayashi S, Matsubara T, Fukuda K, Maeda T, Funahashi K, Hashimoto M, Kamenaga T, Takashima Y and Kuroda R: A genome-wide association study identifying the SNPs predictive of rapid joint destruction in patients with rheumatoid arthritis. *Biomed Rep* 14: 31, 2021.
- Zhang J, Wang N and Xu A: miR-10b-3p, miR-8112 and let-7j as potential biomarkers for autoimmune inner ear diseases. *Mol Med Rep* 20: 171-181, 2019.
- Seguí N, Pineda M, Navarro M, Lázaro C, Brunet J, Infante M, Durán M, Soto JL, Blanco I, Capellá G and Valle L: GALNT12 is not a major contributor of familial colorectal cancer type X. *Hum Mutat* 35: 50-52, 2014.
- Evans DR, Venkitachalam S, Revoredo L, Dohey AT, Clarke E, Pennell JJ, Powell AE, Quinn E, Ravi L, Gerken TA, *et al*: Evidence for GALNT12 as a moderate penetrance gene for colorectal cancer. *Hum Mutat* 39: 1092-1101, 2018.
- Zheng Y, Liang M, Wang B, Kang L, Yuan Y, Mao Y and Wang S: GALNT12 is associated with the malignancy of glioma and promotes glioblastoma multiforme in vitro by activating Akt signaling. *Biochem Biophys Res Commun* 610: 99-106, 2020.
- Wang Y, Yu M, Yang JX, Cao DY, Zhang Y, Zhou HM, Yuan Z and Shen K: Genomic comparison of endometrioid endometrial carcinoma and its precancerous lesions in chinese patients by high-depth next generation sequencing. *Front Oncol* 9: 123, 2019.
- Gibson TM, Wang SS, Cerhan JR, Maurer MJ, Hartge P, Habermann TM, Davis S, Cozen W, Lynch CF, Severson RK, *et al*: Inherited genetic variation and overall survival following follicular lymphoma. *Am J Hematol* 87: 724-726, 2012.
- Cates JMM: The AJCC 8th edition staging system for soft tissue sarcoma of the extremities or trunk: A cohort study of the SEER database. *J Natl Compr Canc Netw* 16: 144-152, 2018.
- Yu S, Zhang Y, Li Q, Zhang Z, Zhao G and Xu J: CLDN6 promotes tumor progression through the YAP1-snaill axis in gastric cancer. *Cell Death Dis* 10: 949, 2019.
- Schindelin J, Arganda-Carreras I, Frise E, Kaynig V, Longair M, Pietzsch T, Preibisch S, Rueden C, Saalfeld S, Schmid B, *et al*: Fiji: An open-source platform for biological-image analysis. *Nat Methods* 9: 676-682, 2012.
- Livak KJ and Schmittgen TD: Analysis of relative gene expression data using real-time quantitative PCR and the 2(-Delta Delta C(T)) method. *Methods* 25: 402-408, 2001.
- Wu Q, Liu HO, Liu YD, Liu WS, Pan D, Zhang WJ, Yang L, Fu Q, Xu JJ and Gu JX: Decreased expression of hepatocyte nuclear factor 4a (Hnf4a)/microRNA-122 (miR-122) axis in hepatitis B virus-associated hepatocellular carcinoma enhances potential oncogenic GALNT10 protein activity. *J Biol Chem* 290: 1170-1185, 2015.
- Zhang L, Gallup M, Zlock L, Chen YT, Finkbeiner WE and McNamara NA: Pivotal role of MUC1 glycosylation by cigarette smoke in modulating disruption of airway adherens junctions in vitro. *J Pathol* 234: 60-73, 2014.
- Gaziel-Sovran A, Segura MF, Di Micco R, Collins MK, Hanniford D, Vega-Saenz de Miera E, Rakus JF, Dankert JF, Shang S, Kerbel RS, *et al*: miR-30b/30d regulation of GalNAc transferases enhances invasion and immunosuppression during metastasis. *Cancer Cell* 20: 104-118, 2011.

31. Beaman EM, Carter DRF and Brooks SA: GALNTs: Master regulators of metastasis-associated epithelial-mesenchymal transition (EMT)? *Glycobiology* 32: 556-579, 2022.
32. Liao YY, Chuang YT, Lin HY, Lin NY, Hsu TW, Hsieh SC, Chen ST, Hung JS, Yang HJ, Liang JT, *et al*: GALNT2 promotes invasiveness of colorectal cancer cells partly through AXL. *Mol Oncol* 17: 119-133, 2023.
33. Park MS, Yang AY, Lee JE, Kim SK, Roe JS, Park MS, Oh MJ, An HJ and Kim MY: GALNT3 suppresses lung cancer by inhibiting myeloid-derived suppressor cell infiltration and angiogenesis in a TNFR and c-MET pathway-dependent manner. *Cancer Lett* 521: 294-307, 2021 (Epub ahead of print).
34. Raghu D, Mobley RJ, Shendy NAM, Perry CH and Abell AN: GALNT3 maintains the epithelial state in trophoblast stem cells. *Cell Rep* 26: 3684-3697.e7, 2019.
35. Lin WR and Yeh CT: GALNT14: An emerging marker capable of predicting therapeutic outcomes in multiple cancers. *Int J Mol Sci* 21: 1491, 2020.
36. Scott E, Hodgson K, Calle B, Turner H, Cheung K, Bermudez A, Marques FJG, Pye H, Yo EC, Islam K, *et al*: Upregulation of GALNT7 in prostate cancer modifies O-glycosylation and promotes tumour growth. *Oncogene* 42: 926-937, 2023.
37. Detarya M, Sawanyawisuth K, Aphivatanasiri C, Chuangchaiya S, Saranaruk P, Sukprasert L, Silsirivanit A, Araki N, Wongkham S and Wongkham C: The O-GalNAcylating enzyme GALNT5 mediates carcinogenesis and progression of cholangiocarcinoma via activation of AKT/ERK signaling. *Glycobiology* 30: 312-324, 2020.
38. Dasgeb B, Leila Y, Saeidian AH, Kang J, Shi W, Shoenberg E, Ertel A, Fortina P, Vahidnezhad H and Uitto J: Genetic predisposition to numerous large ulcerating basal cell carcinomas and response to immune therapy. *Int J Dermatol Venereol* 4: 70-75, 2021.
39. Ou C, Sun Z, He X, Li X, Fan S, Zheng X, Peng Q, Li G, Li X and Ma J: Targeting YAP1/LINC00152/FSCN1 signaling axis prevents the progression of colorectal cancer. *Adv Sci (Weinh)* 7: 1901380, 2019.
40. Yuan Y, Park J, Feng A, Awasthi P, Wang Z, Chen Q and Iglesias-Bartolome R: YAP1/TAZ-TEAD transcriptional networks maintain skin homeostasis by regulating cell proliferation and limiting KLF4 activity. *Nat Commun* 11: 1472, 2020.
41. Kim M, Ly SH, Xie Y, Duronio GN, Ford-Roshon D, Hwang JH, Sulahian R, Rennhack JP, So J, Gjoerup O, *et al*: YAP1 and PRDM14 converge to promote cell survival and tumorigenesis. *Dev Cell* 57: 212-227.e8, 2022.
42. Liu M, Zhang Y, Yang J, Zhan H, Zhou Z, Jiang Y, Shi X, Fan X, Zhang J, Luo W, *et al*: Zinc-dependent regulation of ZEB1 and YAP1 coactivation promotes epithelial-mesenchymal transition plasticity and metastasis in pancreatic cancer. *Gastroenterology* 160: 1771-1783.e1, 2021.
43. Ajani JA, Xu Y, Huo L, Wang R, Li Y, Wang Y, Pizzi MP, Scott A, Harada K, Ma L, *et al*: YAP1 mediates gastric adenocarcinoma peritoneal metastases that are attenuated by YAP1 inhibition. *Gut* 70: 55-66, 2021.



Copyright © 2023 Yu et al. This work is licensed under a Creative Commons Attribution-NonCommercial-NoDerivatives 4.0 International (CC BY-NC-ND 4.0) License.